Homogeneous Bottleneck Model of Matrix-assisted Ultraviolet Laser Desorption of Large Molecules

Akos Vertes*, R. Gijbels
Department of Chemistry, University of Antwerp (UIA), Universiteitsplein 1, B-2610 Wilrijk, Belgium

R. D. Levine*
The Fritz Haber Research Center for Molecular Dynamics, The Hebrew University, Jerusalem 91904, Israel

SPONSOR REFEREE: K. G. Standing, University of Manitoba, Winnipeg, Canada R3T 2N2

The factors affecting the yield of high-mass molecules by matrix-assisted ultraviolet laser volatilization are examined in a simple model. The key material factors appear to be a low heat of sublimation, subcritical concentration of the guest molecules and a high irradiance input in a short time compared to the sublimation induction period. The model is homogeneous in that the energy density is taken to be uniform within the 'hot region' of the matrix. The two competing effects are the rates of energy transfer from the matrix to the guest molecules and the desorption by sublimation. It is the bottleneck for energy transfer to the embedded guest molecules that makes their energy content lag behind that of the matrix. This is particularly the case for an initially cold sample. When a sufficiently high rate of sublimation can be achieved (e.g., using a high-power laser), the guest molecules (or adduct ions) will desorb internally cold and will thus not fragment. Numerical simulations of the sublimation kinetics using realistic laser and material parameters support the conclusions and delineate the ranges of the critical factors.

The introduction of large biomolecules into the gas phase such that their mass-spectrum and fragmentation can be recorded[1] has received a recent impetus. The $m/z = 100\,000$ limit was broken in 1988 using UV laser desorption from specially prepared samples.[2–4] More recently, even higher masses[5–8] were observed and novel ways of preparing samples[7–11] were described. While detection remains a key factor, it is already clear that matrix-assisted laser desorption is a method of considerable promise. In particular, it opens for study the properties and response of isolated large biomolecules. It is appropriate therefore to identify the primary kinetic mechanism for the desorption of intact labile molecules from within a fairly 'hot' matrix.

Our proposed kinetic model is also meant as a guide to future experiments. It is thus important to establish that it does account for the observed success at realistic values of system parameters (and that sufficiently different parameters will not lead to a similar success). The salient experimental features are: A solution of the biomolecule is mixed with an excess (as a concentrated solution or a slurry) of the host matrix material. The resulting mix is deposited onto a metal substrate and dried. The laser irradiation is carried out in vacuum using a short (10–20 ns) pulse in the visible or UV region of the spectrum. The biomolecules are detected as adducts with (small, e.g., H^+ or Na^+) ions. Under optimal conditions, e.g. Table 1, there is no noticeable presence of ions resulting from fragmentation of the biomolecules.

The host molecules noted in Table 1 have a high absorption of the laser light. During the laser pulse, the energy remains fairly localized within the irradiated region. The purpose of our kinetic model is to describe the energy transfer processes during and after the laser pulse. The critical question is how the fragile guest molecules survive in the high-energy-density lattice. Qualitatively, we argue that this is possible due to the 'cooling down' of the lattice by sublimation and due to poor energy transfer to the guest molecules. The rate of evaporation is a very strong (i.e., exponentially increasing) function of the lattice energy density. The faster the energy transfer into the lattice, even faster is the cooling by sublimation. This is favorable due to the slower energy transfer to the guest molecules.

The idea of desorbing internally cold molecules from hot surfaces by fast heating goes back to the early seventies.[12] Further development of the subject was reviewed by several authors.[13] Previous attempts to describe laser/solid interaction include the hydrodynamic model suitable to explain several phenomena at higher irradiances[14] and the surface-heating model devoted to laser-induced thermal desorption situations.[13,15] A bottleneck model was introduced to describe laser-induced bond-selective processes at interfaces[16] and checked by classical molecular dynamic simulations.[17] The advantage of this model is that it is able to account for the desorption of internally cold molecules, rapidly heated by a laser pulse, from a solid surface.

In this paper we will combine the energy-deposition concept[18] with the description of bottlenecks[16] in the homogeneous energy redistribution processes. The nature of these bottlenecks is taken to be due to the poor coupling of the internal modes of guest molecules to the lattice vibrations. We do allow for direct host-to-guest molecular energy transfer. This could lead to

* Authors to whom correspondence should be addressed.

0951-4198/90/0228-0233 $5.00

Table 1. Operating conditions for matrix-assisted UV laser volatization of biomolecules

	Laser			Target				References
Type	Wavelength (nm)	Irradiance (W/cm^2)	Pulse length (ns)	Hosts	Guests	Substrate	M_{max}	
N_2	337	(?)	15	Co powder + glycerol	proteins polymers	metal	~100000	2
4ω-NdYAG	266	10^7–10^8	10	Nicotinic acid	proteins	Al, Ag	~300000	3, 4, 5, 8
Excimer pumped dye	266	10^7	10	Nicotinic acid	proteins	Ag	~150000	6
Excimer pumped dye	581	10^6–10^8	20	Water + buffer	DNA	Cu	~410000	7
4ω-NdYAG	266	5×10^5–10^{-6}	10	Nicotinic acid 2-Pyrazine carboxylic acid Thymine 3-Methoxy-4-hydroxybenzoic acid Thiourea Cinnamic acid	proteins	stainless steel	~116000	9, 10
3ω-NdYAG	355	10^6	10	4-hydroxy-3-methoxycinnamic acid 3,4-dihydroxcinnamic acid 3,5-dimethoxy-4-hydroxy-cinnamic acid	proteins	Pt	~65500	11

rapid heating of the guest, but the lattice vibrations drain the host intramolecular excitation so much more effectively, that the net effect of the direct coupling is not large.

Our qualitative conclusions are then that one should strive for the highest possible rate of sublimation (e.g., by increasing the surface-to-volume ratio) and for sufficiently low concentration of biomolecules. Lowering the guest concentration has the beneficial effect of diminishing the energy transfer to the embedded guest molecules but also leads to lower potential of detecting the volatilized large molecules. Therefore, a trade-off between these two effects should provide the practical value of guest concentration. It is also worth considering the use of a matrix with a high absorption coefficient in the UV which will maintain the power input but with a reduced direct energy transfer to the biomolecules (e.g., by ensuring a frequency mismatch). Of course, such a matrix needs to have a low sublimation temperature.

THE MODEL

In order to follow the path of the deposited energy in the target we partitioned its energy density, ρe, in the following way:

$$\rho e = (1-x)H + L + xG + B \qquad (1)$$

where H, L, G and B denote the energy-density content of the host, the lattice and the guest, and the energy density used for bond-breaking, respectively. x is the volume fraction of the guest molecules.

We take the area of the volume element heated by the laser to be determined by the laser beam cross-section and its thickness by the inverse of the host absorption coefficient, α_{OH}^{-1}. The energy density is increased in this volume by laser heating:

$$\frac{d(\rho e)_{heat}}{dt} = \frac{\alpha_{0H} + \alpha_{0G}}{\sqrt{\pi}} \Phi_0 \exp[-(t-t_0)^2/\tau_p^2. \qquad (2)$$

Here, Φ_0 stands for the laser irradiance, t_0 and τ_p describe the center and the halfwidth of a Gaussian laser pulse and α_{0H} and α_{0G} are the effective absorption coefficients of the host and the guest (weighted by their concentration).

In the power-density regime we are discussing (see Table 1), there are two main mechanisms to cool the excited volume; phase transformation and heat conduction. Inspecting the enthalpies of the possible phase-transition processes we concluded that the two most effective cooling phase transitions are evaporation and sublimation.

Cooling by heat conduction becomes important only on a time-scale much longer than the limit set by the length of the laser pulse and by the rate of the relaxation processes. As an estimate, we consider the time necessary to smear a temperature distribution by heat conduction in an insulator on a scale comparable to the light penetration depth:

$$t_{hc} \approx (4\alpha_{OH}^2 \kappa)^{-1} \qquad (3)$$

Taking $\alpha_{0H} = 4\times10^4\,cm^{-1}$ for nicotinic acid (the most common host) and $\kappa \approx 0.01\,cm^2$ as a typical value for the heat diffusivity of insulating solids, we arrive at $t_{hc} \approx 16$ ns. Because this time is only slightly longer than the laser pulse (see Table 1), at the end of the irradiation too much energy will not have escaped from the region via heat conduction. On the other hand, the resemblance of t_{hc} to τ_p supports the assumption of the uniformly distributed power density. A more elaborate treatment can be based on spatially dependent description of the energy distributions.

Another possible cooling mechanism is[19] 'volume evaporation' due to the energy stored in the thermal expansion of the matrix. This mechanism is known[20] to be important for matter having low absorption of laser radiation. We do not therefore consider it here, but do include it in a future publication which treats infrared laser energy deposition.

The cooling rate, expressed by the phase transition enthalpy, ΔH_{phtr}, and temperature, T_{phtr}, is written as

$$\frac{d(\rho e)_{cool}}{dt} = \alpha_{0H} p_0 \Delta H_{phtr} \frac{\exp[\Delta H_{phtr}(T_L - T_{phtr})/RT_L T_{phtr}]}{\sqrt{2\pi MRT_L}} \qquad (4)$$

where p_0 is the ambient pressure, T_L is the lattice temperature expressed by $T_L = V_M L/C_p$. V_M and C_p are the molar volume and the lattice specific heat of the host with molecular weight M.

To follow the energy redistribution proccesses we introduce the kinetic equations where the energy-exchange terms are proportional to the energy difference[19];

$$\frac{dH}{dt} = \frac{\alpha_{0H}}{\alpha_{0H}+\alpha_{0G}} \frac{d(\rho e)_{heat}}{dt} - \alpha_{HL}(H-L) - \alpha_{HG}(H-G) - \alpha_{HB}H \quad (5)$$

$$\frac{dL}{dt} = \alpha_{HL}(H-L) - \alpha_{LG}(L-G) - \frac{d(\rho e)_{cool}}{dt} \quad (6)$$

$$\frac{dG}{dt} = \frac{\alpha_{0G}}{\alpha_{0H}+\alpha_{0G}} \frac{d(\rho e)_{heat}}{dt} + \alpha_{HG}(H-G) + \alpha_{LG}(L-G) - \alpha_{GB}G \quad (7)$$

$$\frac{dL}{dt} = \alpha_{HB}H + \alpha_{GB}G \quad (8)$$

Here, α_{HL}, α_{HG}, α_{HB}, α_{LG} and α_{GB} are the host/lattice, host/guest, host/bond-breaking, lattice/guest and guest/bond-breaking energy transfer coefficients, respectively. It is assumed that all the processes except bond breaking are reversible.

The physical picture of laser volatilization underlying these equations is the following. The laser radiation electronically excites mostly the host and, with a lower cross-section also the guest molecules. With very fast internal conversion processes (on the ps timescale) the electronic excitation leads to internal vibrational excitation. At a given rate (α_{HL}) these internal vibrations are transferred to lattice vibration and are also channelled directly to guest vibrations (α_{HG}). The lattice is cooled by the phase transformation and transfers energy to the guest molecules (α_{LG}). The guest heating rate is determined by direct light absorption and energy transfer from the lattice and directly from the host molecules. Both the host and the guest molecules are subject to irreversible fragmentation which consumes some part of the energy.

The physics behind our choice of the energy transfer coefficients is presented in Fig.1. Here we show a segment of the embedded guest molecule surrounded by the lattice of the host. The interactions between the particles are schematically represented by springs. We allow for one typical frequency of the intramolecular vibrations of the host, ν_H, and of the guest, ν_G, and for a typical lattice frequency ν_L. (Strictly speaking, these frequencies are better represented by a range of values appearing in the infrared spectra of the host and the guest and in the phonon spectra of the host lattice). See typical values of these parameters in Table 2.

The energy transfer rate coefficients in such a system of oscillators can be expressed as in Ref 16. (There a single guest molecule was absorbed on the surface of the host). The role of the physisorption bond in Ref. 16 is played here by the hydrogen bond between the host and the guest molecules.

$$\alpha_{HL} = \nu_H \exp(-\xi_{HL}) \quad (9a)$$

$$\alpha_{HG} = \nu_H C_G \exp(-\xi_{HG}) \quad (9b)$$

and

$$\alpha_{LG} = \nu_L C_G \exp(-\xi_{LG}) \quad (9c)$$

where C_G is the fractional volume concentration of guest molecules, $C_G = x/(1-x)$, and ξ_{HL}, ξ_{HG} and ξ_{LG} are adiabaticity parameters.[16] It is the appearance of the guest concentration ratio, C_G, in Eqns (9b) and (9c) that leads to its important role as a critical parameter. Too high a value of C_G leads to increased coupling, particularly so for the direct term α_{HG} since ν_H is comparable to ν_G. It is important to emphasize here that the energy transfer is measured by changes in volume energy density of the guest and not by the energy content of a guest molecule. The role of the physisorption bond in Ref 16 is played here by the hydrogen bond between the host and the guest molecules. The adiabaticity parameters are evaluated as in Ref 16,

$$\xi = \pi(\mu\Delta E)^{1/2}/\hbar a \quad (10)$$

where ΔE is the vibrational energy defect, μ is the reduced mass of the hydrogen bond and a is its range parameter. Instead we can also use

$$\xi = (D\Delta E)^{1/2}/\hbar v \quad (11)$$

where D is the strength of the hydrogen bond (D_{HB} in Table 2) and v is its frequency. For ξ_{HL} we use for D the strength of the host/host interaction; (D_{HB} in Table 2). The bond-breaking coefficients are related to the host and guest bond energies D_H and D_G:

$$\alpha_{HB} = \nu_H \exp\left[-\frac{2\pi D_H}{h\nu_H}\right] \quad (12)$$

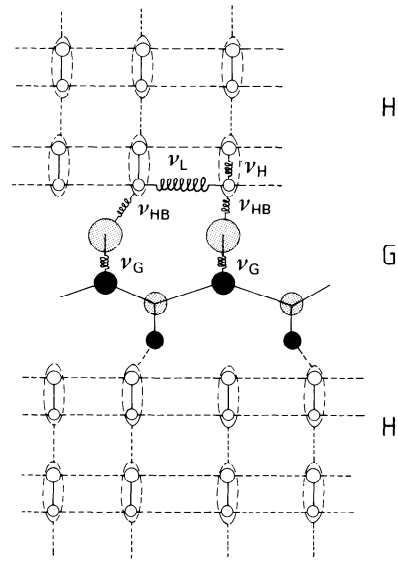

Figure 1. A schematic representation of the three types of vibrational modes which are coupled when a guest (G) molecule is embedded in a lattice of host (H) molecules. Chemical bonds are shown as full lines whereas physical (e.g., H-bonding, dispersion, induction) interactions are shown as broken lines. The springs represent the coupled modes.

Table 2. Laser and material parameters for the case of frequency-quadrupled Nd:YAG laser irradiating a matrix of nicotinic acid (the host) in which protein molecules (the guests) are embedded.

Laser		Target													Ambient	
Φ_0 (W/cm^2)	τ_P (ns)	M (kg/mol)	V_M (cm^3/mol)	C_P (J/mol K)	T_{subl} (K)	ΔH_{subl} (kJ/mol)	C_G (–)	α_{OH} (cm^{-1})	α_{0G} (cm^{-1})	ν_H (s^{-1})	ν_L (s^{-1})	ν_G (s^{-1})	D_{HR} (kJ/mol)	D_{HH} (kJ/mol)	T_0 (K)	p_0 (N/cm^2)
10^7	10	0.123	83.5	150.0	315.0	104.6	10^{-4}	4×10^4	1.0	3×10^{13}	6×10^{12}	2×10^{13}	33	33	300.0	$1.3\cdot10^{-7}$

$$\alpha_{GB} = \nu_G C_G \exp\left[-\frac{2\pi D_G}{h\nu_G}\right] \quad (13)$$

The D's in Eqns (12) and (13) are taken in the computational work to be isomerization barriers (that is, low thresholds) as taking them to be true bond energies will reduce the coupling to unreasonably low values.

To complete the set of differential equations, Eqns (5)–(8), the initial thermal equilibrium is introduced as initial condition:

$$H(t=0) = L(t=0) = G(t=0) = B(t=0) = T_0 C_P / V_M \quad (14)$$

where T_0 is the ambient temperature.

An energy-transfer bottleneck is an extremely low value of one or more of the transfer coefficients. Examining Eqns (9)–(11) it is clear that the host/lattice exchange is much more efficient than the other steps because of the large number of couplings (i.e., α_{HL} is not proportional to C_G). Comparing α_{HG} and α_{LG}, one expects more efficient transfer through direct host/guest coupling, because the host and guest vibrational frequencies can fall in the same region. Therefore the energy-transfer bottleneck is expected at the lattice/guest coupling step and depending on guest concentration also at the host/guest direct coupling. It seems to us that further reducing these two transfer rates can be achieved beyond what is currently the case. The computational results suggest that this is a worthwhile direction for further experimental work.

RESULTS AND DISCUSSION

The solution of Eqns (2) and (5)–(8) was obtained by a standard numerical integration procedure. A typical set of input parameters is depicted in Table 2. The data on target properties are those of nicotinic acid or, if not available (e.g., ν_L), values for other molecular solids were used.

A detailed presentation of the results obtained for the typical parameters is given in Fig 2. The essential information is contained in Fig. 2(b). The same information is repeated in Fig. 3 for non-typical values of different parameters.

The striking result in Fig. 2 is that on the timescale of interest, the lattice energy density (L) is equilibrated with the host (H), while the energy in the biomolecules is significantly lower. There is no discernible bottleneck in the energy transfer to the lattice while there is one to the guest biomolecules.

The time evolution is governed by two rates shown in Fig. 2(a). One is the rate of energy input via the absorption of laser radiation (cf. Eqn (2)). t_0 is the time of peak power of the laser pulse. Already before t_0 the host and lattice are vibrationally quite hot. (The vibrational temperature at the peak exceeds 700 K.) Once the lattice is hot, the rate of sublimation (Fig. 2(a) and Eqn (4)) speeds up, thereby cooling the lattice. This rapid energy (and material) loss is an essential ingredient in our proposed mechanism.

The time at the maximal rate of volatilization is indicated in Fig. 2. During the time interval of rapid material transfer to the gas phase, the guest biomolecules are still fairly cold (i.e., their energy content has

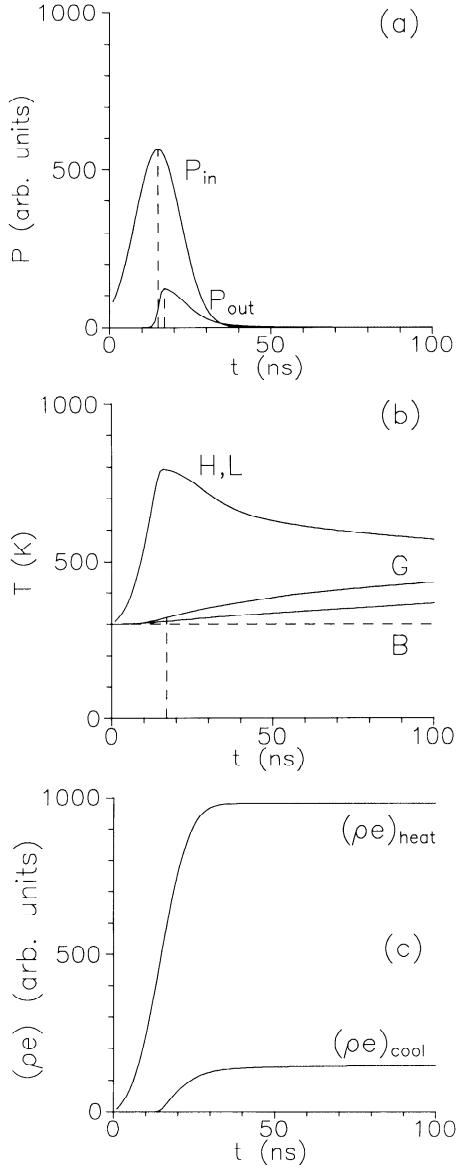

Figure 2. Time history of the energy deposition in the different modes for typical experimental conditions. (a) Shows the input and output (due to evaporation) energy fluxes. Note the time lag between the laser pulse and the evaporation. (b) is the energy density in the host (H), lattice vibration (L), guest biomolecules (G) and thermally degraded guest biomolecules (B). Note that on the time scale shown, the lattice is equilibrated with the host. The rapid rise in H or L causes an evaporation spike which immediately cools the matrix. During much of the evaporation (dashed vertical line) the guest molecules remain internally cold and undegraded. The dashed horizontal line extends the initial temperature (room temperature here) as a reference. (c) is the time-integrated power input and output. See text for further details.

not increased much above its initial value indicated by the dashed horizontal line). This is the quantitative statement of our model; for typical laser and material parameters as given in Table 2, the biomolecules in the gas phase will have a mean vibrational energy not much above its initial value.

If we continue to examine the time evolution well beyond the regime shown in Fig. 2, all the constitutents of the solid matrix will reach equilibrium. The biomolecules embedded in the matrix can then be quite warm and can undergo thermal rearrangement. However, this long timescale is not relevant to the biomolecules in the gas phase since the rate of sublimation has become, by that time, nearly negligible, cf. Fig. 2(a, c). It should also be recognized that our model does not allow explicitly for heat conduction. At these longer times, heat transfer away from the irradiated volume will further cool both the matrix and the guests.

Figure 3 shows that the model not only predicts the desorption of internally cold biomolecules for the right conditions but also the heating up of the biomolecules for the non-optimal conditions. Shown are three distinct studies. In each, the parameters are as in Fig. 2 except as otherwise indicated. Figure 3(a) is for a higher ($C_G = 10^{-2}$) biomolecules concentration relative to the matrix material. This results in a more efficient direct host/guest vibrational energy transfer (cf. Eqn (10)). The guest biomolecules become quite warm and the energy available for sublimation is much reduced. The amount of vaporized material is lower and most of the biomolecules in the gas phase will be warm. The kinetic importance of the heating of the biomolecules can be estimated using an Arrhenius temperature dependent rate coefficient. Even for low threshold energies for thermal degradation, the half-life below 500 K can exceed the 100 ns time scale shown in the Figure.

In Fig. 3(b) the matrix is taken to have a higher sublimation temperature ($T_{sub} = 400$K). The host and lattice are heated by the laser and stay warm. Despite the bottleneck, the high energy density in the matrix results in some heating of the desorbing biomolecules. In terms of our energy redistribution model it is also possible to understand why sublimating matrices are favored over melting matrices. In a melt the dynamically changing local environment of the guest molecules can enhance the energy transfer to the guest. This condition, however, does not exclude melting matrices from the list of possible candidates. If the melting temperature is low enough, the increased efficiency of energy transfer in the melt should not necessarily lead to the fragmentation of the guest molecules.

Heating up and extensive thermal degradation of the biomolecules occurs (Fig. 3(c)) for a longer-lasting laser pulse ($\tau_p = 50$ ns; $\Phi_0 = 2 \times 10^6$ W/cm^2, even though the total energy input is kept at the same values as in Fig. 2). Note however that many of the desorbing biomolecules are not so warm. It is mostly the molecules that remain embedded within the matrix that are degraded. Slow energy coupling to the matrix is doubly detrimental. The cooling is far slower and the coupling to the guest molecules is longer-acting. The desired effect (i.e., lukewarm guest molecules escaping from a hot matrix) is thus due to a separation of time scales and would therefore be absent in steady state.

The results shown in Figs 2 and 3 and other computations suggest that the fundamental kinetic competition is between cooling by evaporation and energy transfer to the biomolecules (primarily by direct transfer from the host molecules).

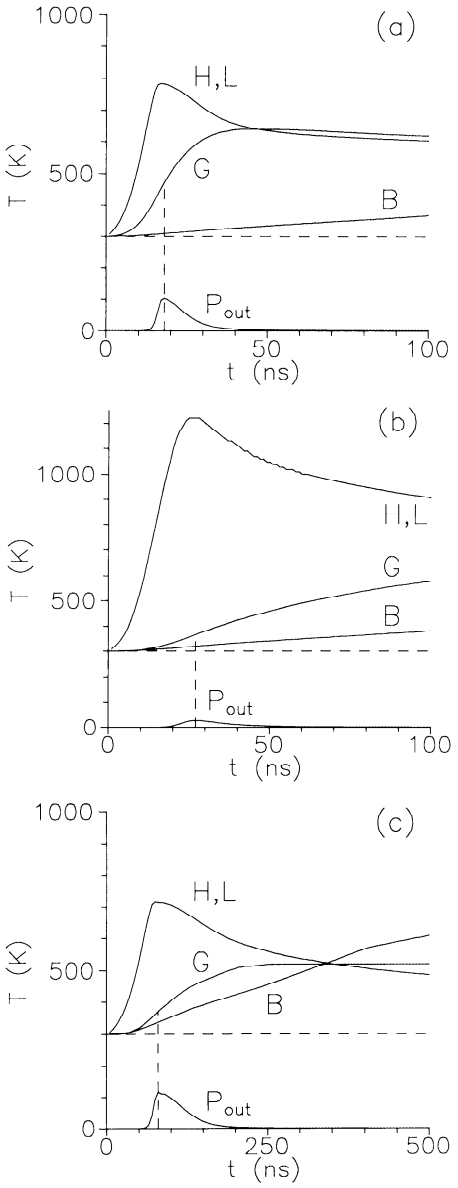

Figure 3. The host (H), lattice (L), guest biomolecules (G) and thermally degraded biomolecules (B) energy content vs time for atypical experimental conditions. (a) Higher guest concentration resulting in more extensive warming of the guest. (b) A higher sublimation temperature of the matrix resulting in far less evaporation. (c) Lower laser power but longer pulse (note change in time scale) such that the total energy input remains the same. Note the extensive thermal degradation. The results in this figure are to be compared to Fig. 2(b). (The sets of parameters are identical in these two figures except $C_G = 10^{-2}$ in (a), $T_{sub} = 400$ K in (b) and $\tau_p = 50$ ns and $\Phi_o = 2 \times 10^6$ W/cm^2 in (c). See text for further details.

Conclusion

The biomolecules are heated by energy transfer from the lattice and the host molecules, primarily the former, with a rate (cf. Eqn (7))

$$\text{rate} = \alpha_{HG}(H - G) + \alpha_{LG}(L - G) \qquad (15)$$

and are desorbing by a rate determined by Eqn (4). The successful experiment will seek to maximize the latter while minimizing the former. In addition to controlling

the rate, one can also gain by starting with a lower initial energy content of the biomolecules. While cooling the matrix needs additional effort, one must remember that the transfer rates add up to the initial energy content. In our computations, the effect of energy transfer is almost additive. (It is not exactly additive due to the (H − G) and (L − G) terms in Eqn (15)). In terms of controlling the rates, one can reduce the energy transfer by (i) keeping the guest concentration as low as practicable (energy transfer vs detectability), (ii) using a matrix host molecule with as poor a frequency overlap with the frequencies of the biomolecule as possible. One can enhance the volatilization rate by (iii) using a host matrix with a low sublimation temperature and (iv) using a laser pulse short enough to promote volatilization instead of degradation.

Acknowledgements

We thank Profs. J. Grotemeyer and E. W. Schlag for discussions. The Fritz Haber Research Center is supported by the Minerva Gessellschaft für die Forschung, mbH, Munich, BRD.

REFERENCES

1. See for example: J. Grotemeyer and E. W. Schlag, *Angew. Chem.* (Int. Ed. Engl.) **27**, 447 (1988) or articles in "*Mass Spectrometry in the Analysis of Large Molecules*", Ed. by C. J. McNeal, Wiley, Chichester (1986).
2. K. Tanaka, H. Waki, Y. Ido, S. Akita, Y. Yoshida and T. Yoshida, *Rapid Commun. Mass Spectrom.* **2**, 151 (1988).
3. M. Karas and F. Hillenkamp, *Anal. Chem.* **60**, 2299 (1988).
4. M. Karas, U. Bahr and F. Hillenkamp, *Int. J. Mass Spectrom. Ion Proc.* **92**, 231 (1989).
5. J. Grotemeyer and E. W. Schlag, private communication (1990).
6. M. Salehpour, I. Perera, J. Kjellberg, A. Hedin, M. A. Islamian, P. Hakansson and B. U. R. Sundqvist, *Rapid Commun. Mass Spectrom.* **3**, 259 (1989).
7. R. W. Nelson, M. J. Rainbow, D. E. Lohr and P. Williams, *Science* **246**, 1585 (1989).
8. M. Karas, U. Bahr, A. Ingendoh and F. Hillenkamp, *Angew. Chem.* (Int. Ed., Engl.) **28**, 760 (1989).
9. R. C. Beavis and B. T. Chait, *Rapid Commun. Mass Spectrom.* **3**, 233 (1989).
10. R. C. Beavis and B. T. Chait, *Rapid Commun. Mass Spectrom.* **3**, 432 (1989).
11. R. C. Beavis and B. T. Chait, *Rapid Commun. Mass Spectrom.* **3**, 436 (1989).
12. R. J. Beuhler, E. Flanigan, L. J. Greene and L. Friedman, *J. Am. Chem. Soc.* **96**, 3990 (1974).
13. See for example: F. Hillenkamp, in "*Ion Formation from Organic Solids*", Ed. by A. Benninghoven, Springer Series in Chemical Physics, **25**, p. 190, Springer-Verlag, Berlin (1983). Or; A. N. Shibanov, in "*Laser Analytical Spectrochemistry*", p. 353, Ed. by V. S. Letokhov, Adam Hilger, Bristol (1986).
14. A. Vertes, P. Juhasz, M. De Wolf and R. Gijbels, *Int. J. Mass Spectrom. Ion Proc.* **94**, 63 (1989).
15. A. Vertes, P. Juhasz, L. Balazs and R. Gijbels, *Microbeam Analysis* 273 (1989).
16. R. N. Zare and R. D. Levine, *Chem. Phys. Letters* **136**, 593 (1987).
17. T. A. Holme and R. D. Levine, *Surf. Sci.* **216**, 587 (1989).
18. A. Vertes, P. Juhasz, M. De Wolf and R. Gijbels, *Scanning Microscopy* **II**, 1853 (1988).
19. A. Vertes and R. D. Levine, to be published.
20. M. von Allmen, "*Laser-Beam Interactions with Materials, Physical Principles and Applications*" p. 152, Springer-Verlag, Berlin (1987).

Received 27 April 1990, accepted 28 April 1990.